Colloid Polym Sci (2002) 280: 1001–1008
DOI 10.1007/s00396-002-0719-7

ORIGINAL CONTRIBUTION

Tsuneo Okubo
Keisuke Kimura
Hiroshi Kimura

Dissipative structures formed in the course of drying the colloidal crystals of monodispersed polystyrene spheres on a cover glass

Received: 1 March 2002
Revised: 4 April 2002
Accepted: 12 April 2002
Published online: 3 July 2002

Presented at the Annual Meeting of the Society of Fiber Science and Technology, Japan, Kyoto, June 7–9, 2000

T. Okubo (✉) · K. Kimura · H. Kimura
Department of Applied Chemistry and Graduate School of Materials Science, Gifu University, Gifu 501–1193, Japan
E-mail: okubotsu@apchem.gifu-u.ac.jp
Fax: +81-58-293-2628

Abstract Macroscopic and microscopic dissipative structural patterns formed in the course of drying the deionized aqueous colloidal crystal suspensions of monodispersed polystyrene spheres (diameter: 88 nm) on a cover glass have been observed. Spoke-like and ring-like crack patterns are formed in the macroscopic scale. The broad ring patterns of the hill accumulated with spheres are also formed around the outside edge. The pattern area, drying time, neighbored inter-spoke angle, thickness of the film, and other morphological parameters have been discussed as a function of sphere concentration and concentration of sodium chloride. Fractal patterns of the sphere association are observed at the microscopic scale. Capillary forces between spheres at the air-liquid surface and the relative rates of water flow at the drying front and the convection flow of water accompanying the movement of spheres are important for the pattern formation.

Keywords Dissipative structure · Pattern formation · Drying colloidal crystal suspensions · Polystyrene spheres · Fractal pattern

Introduction

It is well known that most patterns in nature and in experiments in the laboratory are formed via self-organization in the course of dissipation of free energy and in the non-equilibrium state. Among the many factors for the free-energy dissipation, evaporation and the convection induced by the earth's gravity would be very important for the pattern formation.

Colloidal crystallization phenomena in a closed container (which are not dissipative structures but typical examples of three-dimensional self-organization in the thermodynamic equilibrium state) have been studied intensively by many researchers including the authors' group [1, 2, 3, 4, 5, 6, 7, 8, 9, 10]. It has been clarified that the structural and kinetic properties of colloidal crystals are influenced strongly by the electrostatic inter-particle repulsion via the electrical double layers around the particles, by the shape of colloidal particles, and by the interaction between the particles and the cell wall of a sample container. For example, the most dense crystal planes, 111 and 100 crystal planes for the face-centered-cubic (fcc) and body-centered-cubic (bcc) lattices, always orient parallel to the cell wall [11]. Furthermore, colloidal crystallization rates are much higher for the plane cell than those for the curved tube cell [11].

Several papers on the pattern formation in the course of drying of the monodispersed colloidal suspensions have been reported so far [12, 13, 14, 15, 16, 17, 18, 19, 20, 21, 22, 23, 24, 25, 26, 27]. Most of the papers have studied the liquid-like suspensions containing more or less ionic species. As the important factors of dissipative structures, electrostatic inter-particle interactions have been pointed out. Hydrophobic and hydrophilic interactions are also demonstrated to be important for the drying process [17, 25, 26]. Gelbart et al. [15, 16, 18] examined the mechanism of solvent dewetting in annular

ring structures formed by drying a diluted metal colloid on a substrate. Shimomura et al. have studied intensively the dissipative patterns in the processes of film formation by drying the polymer solutions [28].

In a previous paper from our laboratory [29], the dissipative patterns have been observed in the course of drying colloidal crystal suspensions of silica spheres, which are hydrophilic in their surfaces, on a cover glass. The colloidal crystals are undoubtedly one of the most simple and convenient systems for study of the dissipative structures on laboratory scale. For example, the structural information in the processes of the dissipative pattern formation from the colloidal crystal suspensions is available from the reflection spectroscopy in real time and in detail. In this work, the experiments concerned the colloidal crystals of hydrophobic polystyrene spheres in order to study what patterns are common and/or special for each colloidal sphere.

Experimental

Materials

Monodispersed polystyrene spheres, D1W52 were manufactured by Dow Chemical (Indianapolis, IN). The diameter, standard deviation (δ) from the mean diameter, and the polydispersity index (δ/d_o) were 88 nm, 6.2 nm, and 0.07, respectively. The colloidal sample was first purified several times using an ultrafiltration cell (Model 202, Diaflo-XM300 membrane, Amicon), and then deionized by coexistence with a mixed bed of cation- and anion-exchange resins [Bio-Rad, AG501-X8 (D), 20–50 mesh] for more than seven years before use. They released an amount of alkali from their surfaces. It takes such a long time before complete deionization is achieved because the deionization proceeds between the two solid-liquid phases one after another, i.e., between colloidal spheres and water and then between water and the resins. The surface density of strongly acidic and weakly acidic charges of these spheres were determined to be 1.14 $\mu C/cm^2$ and 1.7 $\mu C/cm^2$ by the conductometric titration with a Horiba Model DS-14 conductivity meter (Kyoto).

The water used for the sample preparation was purified by a Milli-Q reagent grade system (Milli-RO5 plus and Milli-Q plus, Millipore, Bedford, Mass.).

Observation of the dissipative structures

Samples of 0.05 ml to 0.2 ml of the aqueous suspension of D1W52 spheres were dropped carefully and gently onto a micro cover glass (30 mm×30 mm, thickness No.1, 0.12 to 0.17 mm, Matsunami Glass, Kishiwada, Osaka) in a schale (60 mm in diameter, 15 mm in depth, Petri, Tokyo). The cover glass was used without further rinsing in this work. The extrapolated value of the contact angle for pure water was $31 \pm 0.2°$ from the drop profile of a small amount of water (0.2, 0.4, 0.6, and 0.8 µl) on the cover glass. A pipette (1 ml, disposable serological pipette, Corning Lab. Sci.) was used for the dropping. Macroscopic and microscopic observation was made of the film formed after the suspension was completely dried on the cover glass in a room air-conditioned at 25 °C and 65% humidity of the air. Concentrations of the colloidal spheres and sodium chloride ranged from 8.9×10^{-9} to 0.066 in volume fraction and from 1×10^{-6} mol/l to 1×10^{-4} mol/l, respectively.

Macroscopic dissipative structures were observed with a digital HD microscope (type VH-7000, Keyence, Osaka) and a Canon EOS 10 camera with macro-lens (EF 50 mm, f = 2.5) and a life-size converter EF. Microscopic structures were observed with a laser 3D profile microscope (type VK-8500, Keyence) and a metallurgical microscope (Axiovert 25CA, Carl-Zeiss, Jena). Observation of the microscopic patterns was also made with an atomic force microscope (type SPA400, Seiko Instruments).

Reflection spectroscopy

Reflection spectra were taken perpendicularly to the colloidal films developed on a cover glass. A light beam from a halogen lamp (Hayashi LA-150SX, Tokyo) hits the sample using a Y-type optical fiber cable and the reflected light is measured on a multi-channel photo detector (type MCPD-7000G3, Otsuka Electronics, Hirakata, Osaka).

Results and discussion

Macroscopic patterns

Figure 1 shows the typical patterns formed in drying the suspensions of D1W52 spheres at sphere concentrations ranging from 8.85×10^{-6} to 0.0221 in volume fraction. At low sphere concentrations, several fine circles and/or islands of sphere regions distributed roundly in the outer regions. On the other hand, at high sphere concentrations of 0.0199 and 0.0221 in volume fraction, the spoke-like cracks were formed from the outside edge toward the center. Surprisingly, these macroscopic patterns for polystyrene spheres are very similar to those observed for the colloidal silica spheres [29], though the former are hydrophobic from the styrene groups at the colloidal surface and differ from the latter that are hydrophilic from the silanol groups. Clearly, the cracks were formed in the process of shrinkage of the wetted films [29, 30, 31]. For polystyrene sphere systems, several macroscopic cracks at right angles to the spoke-like cracks were also observed, as is clear in Fig. 1d. These ring-like cracks were not observed for colloidal silica spheres [29]. There remained few spheres in the central region, whereas the broad ring-like region was occupied with a large number of the spheres in the outside region of Figs. 1c and d. Broad ring patterns became narrow when sphere concentration decreased as is shown in Figs. 1c and d. It should be mentioned here that the macroscopic spoke-like and the broad ring patterns were also observed for the deionized aqueous suspensions of India ink [32].

A main cause for the broad ring formation is due to the convection flow of the solvent and the colloidal spheres. Especially important is the flow of the colloidal spheres from the center area toward the outside edges in the lower layer of the liquid drop, which was observed directly from the movement of the very rare aggregates of the spheres [29]. The flow is enhanced by the evaporation of water at the liquid surface, resulting in lowering of the suspension temperature in the upper region. When the spheres reach the edges of the drying frontier at the outside region of the liquid, a part of the spheres

will turn upwards and go back to the center region. However, the movement of most spheres may stop at the frontier region because of the disappearance of water. This process must be followed by the broad ring-like accumulation of the spheres near the round edges. It should be noted here that the importance of the convection flow of colloidal spheres in the ring formation has been often reported in the process of film formation [20, 33].

The area (S) of the dried film agreed with that of the initial state of the drop when the sample liquid with sphere concentrations higher than 0.01 in volume fraction (ϕ) was set on a cover glass. The S-values shown in Fig. 2 with other parameters increased slightly as ϕ increased. This is beautifully interpreted by the slight decrease in surface tension of polystyrene sphere suspensions as sphere concentration increases [34]. The angles between the adjacent spoke-like cracks (θ) increased as sphere concentration increased. The θ-values correlate deeply with the convection flow of water and then of the spheres, as described above, and further with the rigidity of the dried film separating from the cover glass. Interestingly,

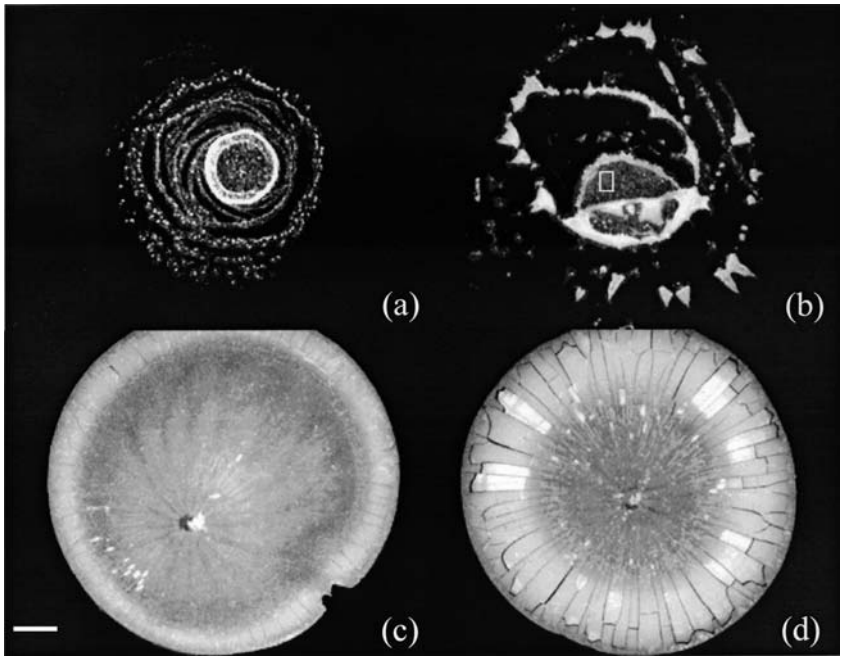

Fig. 1. Patterns formed for D1W52 spheres on a cover glass at 25 °C. (*a*) $\phi = 8.85\times10^{-6}$, (*b*) 8.85×10^{-4}, (*c*) 0.0199, (*d*) 0.0221. In water, 0.1 ml, length of the bar is 1.0 mm

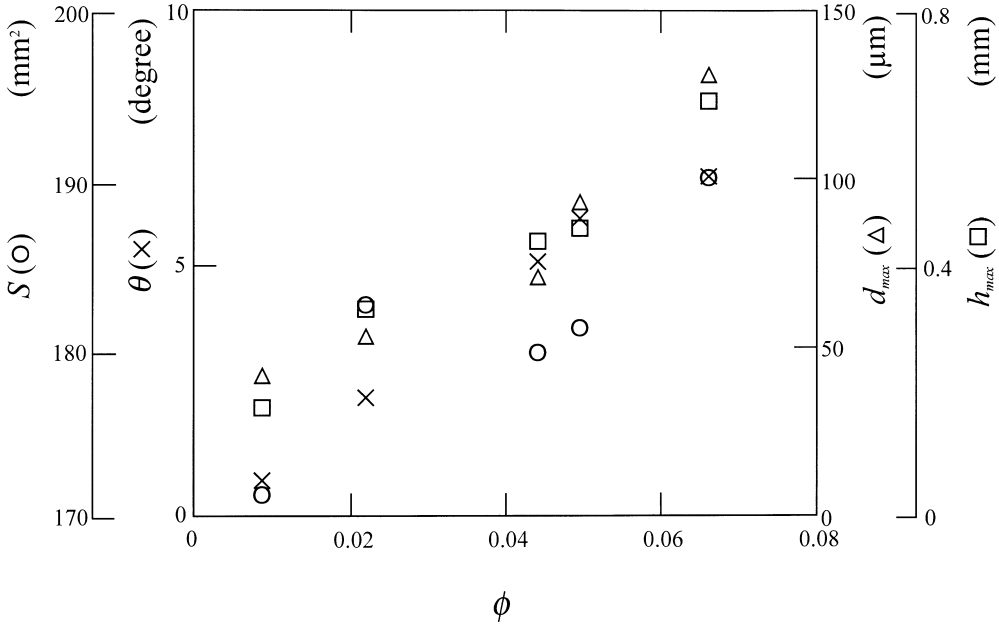

Fig. 2. The S, θ, d_{max} and h_{max} values of D1W52 spheres as a function of sphere concentration at 25 °C. In water, 0.2 ml

the cracks were introduced in the final stage of drying the colloidal suspensions along the outer edges first, where the dryness proceeds in advance. Then the cracks curved and then developed straight toward the center of the film. It is impressive that the new cracks developed successively keeping the same angle with the adjacent old cracks. The θ-value should increase as the rigidity of the wetted film increases. It should be noted here that the θ-values increased as the sphere concentration of the suspension drop increased, as is clear in Fig. 2. This observation can also be explained by the increased rigidity of the film, since the area of the film increased only slightly as the sphere concentration increased.

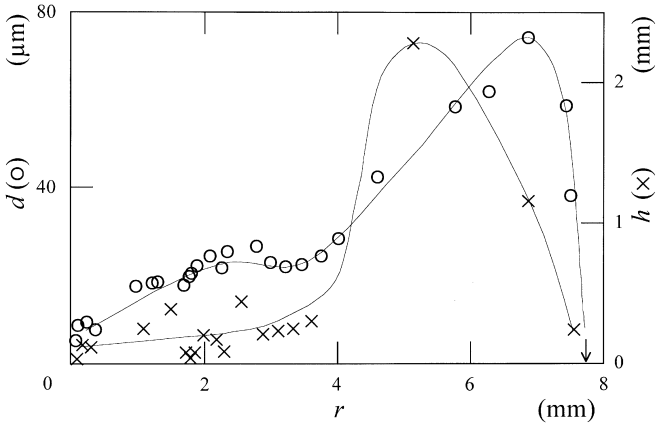

Fig. 3. Thickness of the film and the width between the neighboring circle cracks formed for D1W52 spheres as a function of the distance from the center at 25 °C. In water, $\phi = 0.0221$, 0.2 ml

The thickness of the film (d) is shown in Fig. 3 as a function of the distance from the center, r. An arrow shows the outer edge of the film formed. The measurements were made using the laser microscope. Clearly, film was thickest in a part slightly in from the outside edge and thinnest in the center, as has been discussed above. The distances of the neighboring ring-like crack (h) are also shown as a function of r in Fig. 3. Interestingly, profiles of the r-dependencies of h and d are quite similar to each other. The maxima in the d-values, d_{max} and in the h-values, h_{max} increased as sphere concentration increased as is shown in Fig. 2.

Figure 4 shows the influence of salt on the macroscopic patterns. Clearly, the shape of the outer edge changed greatly from smooth to rough with the addition of sodium chloride, which is quite similar to silica spheres [29]. The reason for this observation is not clear yet. A slight increase in the air-suspension interface tension by the addition of sodium chloride to the suspension will be one of the main reasons. Table 1 shows the influence of the salt concentration on several parameters. The time for completion of the drying observed with the naked eye, T, increased significantly with the addition of NaCl. It should be noted that the film at time T is still wet and not dried completely, as will be discussed in the section on reflection spectrum measurements. Interestingly, the area (S) decreased in the presence of sodium chloride. This is explained by the increase of surface tension in the presence of sodium chloride. The θ-values increased greatly with the addition of sodium chloride. This is also quite similar to the observation for colloidal silica spheres [29] and is due to

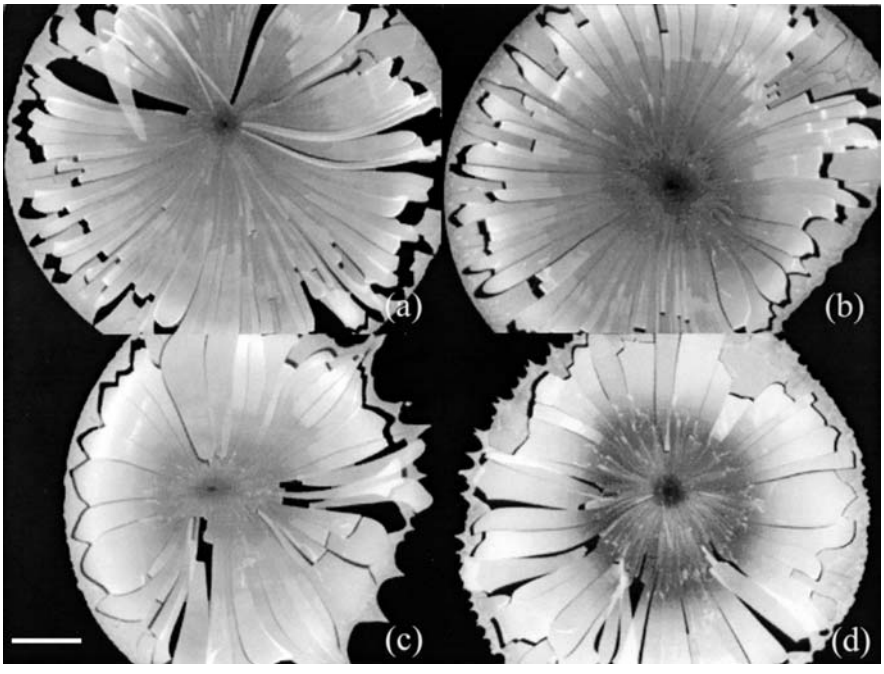

Fig. 4. Patterns formed for D1W52 spheres in the presence of sodium chloride on a cover glass at 25 °C. In water, $\phi = 0.0221$, 0.2 ml. (*a*) [NaCl] = 0 mol/l, (*b*) 1×10^{-5} mol/l, (*c*) 1×10^{-4} mol/l, (*d*) 1×10^{-3} mol/l. Length of the bar is 2.0 mm

Table 1. Influence of salt on T, S, θ, d_{max}, and h_{max}. $\phi = 0.0221$, 0.2 ml

[NaCl] (mol/l)	T (min)	S (mm^2)	θ (degree)	d_{max} (μm)	h_{max} (mm)
0	216	183	2.3	63	0.3
1×10^{-5}	267	142	4.3	93	2.7
1×10^{-4}	282	106	9.0	127	3.0
1×10^{-3}	258	122	9.1	100	4.1

the decrease in the nearest-neighbored inter-sphere distance with sodium chloride through thinning of the electrical double layers around colloidal spheres followed by an increase in the elastic modulus of the film. It should be mentioned further that the d_{max} values increased with the addition of sodium chloride. The reason for this observation is not clear yet. The h-values also increased substantially as the salt concentration increased.

Microscopic patterns

Figure 5 shows the typical patterns observed for the films from suspension of comparatively low sphere concentration at $\phi = 8.85\times10^{-4}$. White parts are occupied with the colloidal spheres and the black regions are vacant of spheres on a cover glass. These microscopic patterns seem to be fractal. These patterns must be made by the movement of spheres to associate with each other, especially in the final stage of the drying processes. The atomic force microscope observation clarified that a large number of colloidal spheres associate on a cover glass making the fractal pattern, though the picture showing this was omitted in this report. The driving force for the association will be the van der Waals and further hydrophobic inter-sphere attraction. This is because the sphere concentration in the final stage is extremely high, even close to the close-packing concentration (0.72 in volume fraction) and the inter-sphere surface distances become very close. The concentrations ranging from 4×10^{-4} to 4×10^{-3} in volume fraction were most appropriate for formation of the fractal patterns. The fractal dimensions of the patterns, estimated by counting the number of squares covering colloidal spheres [35], were 1.45 irrespective of the sphere concentration. These values are similar to those of colloidal crystals of silica spheres, between 1.3, and 1.9 [29], and slightly larger than the fractal dimension of Koch curve, 1.26.

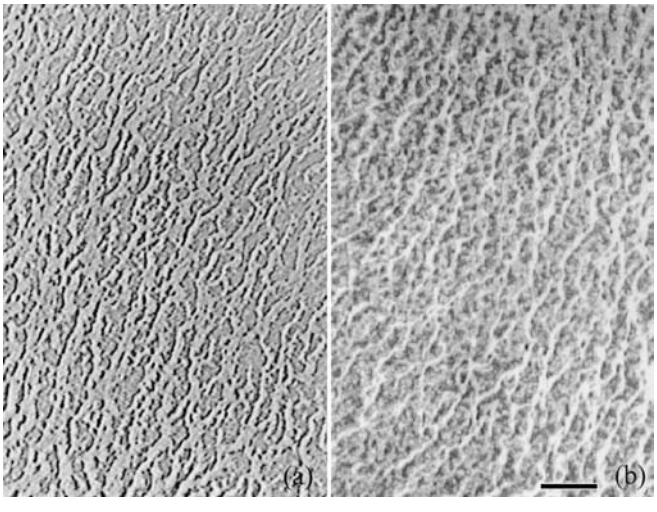

Fig. 5. Patterns formed for D1W52 spheres on a cover glass at 25 °C. In water, $\phi = 8.85\times10^{-4}$, 0.1 ml. (*a*) by metallurgical microscope, (*b*) laser microscope. Length of the bar is 10 μm

Reflection spectroscopy in the course of drying

Interestingly, the single crystals were observed whole during the drying processes. Figure 6 shows the close-up color pictures of the single crystals appearing in the center region at $t = 0$ min, 20 min, 100 min, and 120 min. The drying time, T, was 190 min for this system. At time T, the film looked completely dry to the naked eye. However, the peak wavelength of the film in the reflection spectroscopy at $t = T$ was larger than that of the completely dried film at $t = 12$ days, as is described below. This fact indicates that the film at $t = T$ is still wet and some water is included in the vacancies of the film. These films at $t = T$ are, therefore, called "wet" film in this work. The size of the single crystals increased in the course of drying, which clearly shows that the

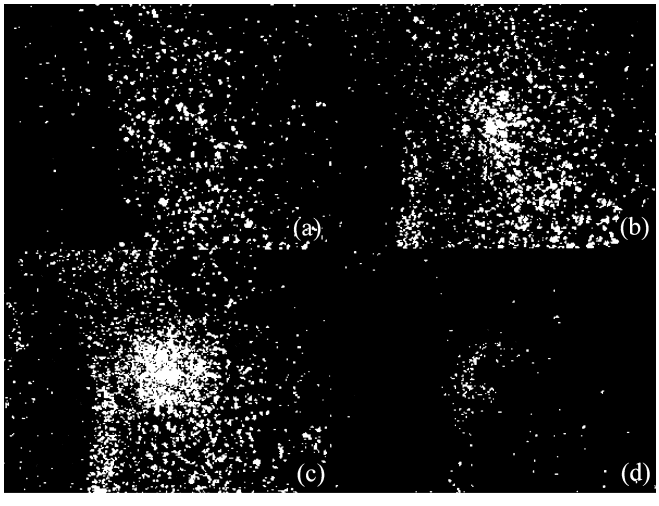

Fig. 6. Single crystals observed in the drying process of D1W52 spheres on a cover glass at 25 °C. In water, $\phi = 0.0332$, 0.05 ml, $r = 0$ mm. (*a*) $t = 0$ min, (*b*) 20 min, (*c*) 100 min, (*d*) 120 min. Length of the bar is 200 μm

contamination of the suspensions with air, especially with carbon dioxide, progresses with time. It is well known that the crystal size becomes largest at the salt concentration slightly lower than the critical salt concentration of crystal melting [10, 11]. The crystal size began to decrease after passing the maximum as time proceeded. This is ascribed to the decrease in the crystal size as sphere concentration further increases. The single crystals were not recognized in the wet drying state at $t = 190$ min. However, the peak appeared even for the wet film and for the completely dried film after 12 days in the reflection spectroscopy, as will be described below.

It should be mentioned here that the drying time (T) was shown to be sensitive to the room temperature and humidity, amount of liquid drop, sphere concentration, ionic concentration, and the degree of rinse of a cover glass. The mean evaporation rates of water in the course of drying were estimated from the T-values, and ranged from 0.23 μl/min to 0.93 μl/min.

Figure 7 shows the reflection spectra in the course of drying at the center of the pattern. The peak wavelength (λ_p) decreased with time, especially drastically in the final stage of drying between 160 min and 180 min, as is clear in Table 2. It should be noted here that the λ_p values at $r = 2.7$ mm and 3.5 mm shifted slightly to the longer wavelengths at the beginning stage of drying, as is shown in Table 2. These observations show that the sphere concentration decreases slightly at the initial stage and then increases. Just before completion of drying at the center, the reflection spectra become broad. However, the reflection peaks remained even at the state of dryness at $t = 180$ min. These observations clearly show that almost all the spheres at the center

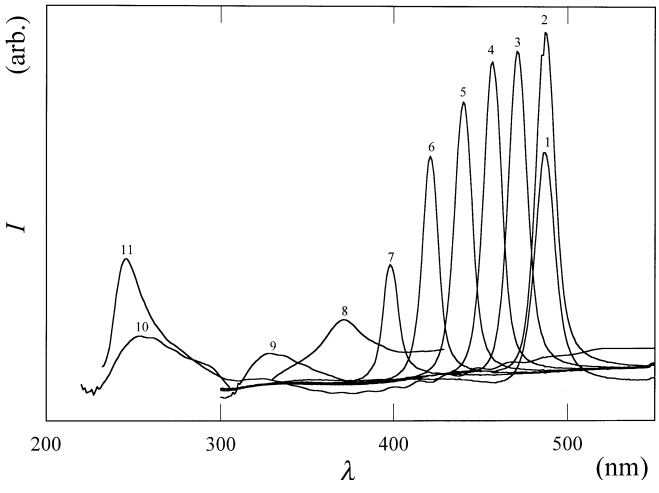

Fig. 7. Reflection spectra of the film formed for D1W52 spheres on a cover glass at 25 °C. In water, $\phi = 0.0332$, 0.05 ml, $r = 0$ mm. *Curve* (*1*) $t = 0$ min, (*2*) 20 min, (*3*) 40 min, (*4*) 60 min, (*5*) 80 min, (*6*) 100 min, (*7*) 120 min, (*8*) 140 min, (*9*) 160 min, (*10*) 180 min, (*11*) 12 days

Table 2. Change in the reflection peak wavelength and the nearest-neighbored intersphere distance in the course of drying of D1W52 spheres from reflection spectroscopy. $\phi = 0.0332$, $r = 0$ mm, 0.05 ml, $T = 190$ min

	$r = 0$ mm		$r = 2.7$ mm		$r = 3.5$ mm	
t (min)	λ_p (nm)	l_{obs} (nm)	λ_p (nm)	l_{obs} (nm)	λ_p (nm)	l_{obs} (nm)
0	489	225	478	220	482	222
20	485	224	480	221	473	218
40	471	217	469	216	456	210
60	457	210	457	211	437	201
80	440	203	438	202	422	194
100	422	194	422	194	406	187
120	398	183	401	185	393	181
140	372	171	379	175	370	170
160	324	149	357	164	351	162
180	257	118	243	112	239	110

region go away towards the outside by convection flow. It is interesting to note that the dried film still shows the reflection peaks indicating the existence of the crystal-like structures in the film. The crystal-like arrangement of polystyrene spheres that had dried completely in a cover glass has been reported in a previous paper [36].

The most reliable inter-sphere distances (l_{obs}) were obtained in Table 2 by the repeated calculations from the observed λ_p value and the old n value using Eq. 1 and Eq. 2.

$$l_{obs} = 0.6124\lambda_p/n \tag{1}$$

$$n = \phi \times [\text{refractive index of polystyrene}] + (1 - \phi) \times [\text{refractive index of water or air}] \tag{2}$$

Here, the refractive indices of polystyrene, water, and air were assumed to be 1.7, 1.33, and 1.0, respectively.

The λ_p and l_{obs} values for the completely dried films at $r = 0$ mm and at $t = 12$ days are compiled in Table 3. Clearly, the l_{obs} values at $r = 0$ mm decreased from the initial one of 225 nm at $\phi = 0.0332$ to that of the completely dried film, i.e., 98.8 nm as is shown in Tables 2

Table 3. Reflection peak wavelength and the nearest neighbored intersphere distance of the completely dried film of D1W52 spheres at $t = 12$ days from reflection spectroscopy. $\phi = 0.0332$, $r = 0$ mm, 0.05 ml

ϕ	T (min)	λ_p (nm)	l_{obs} (nm)
0.00088_5	219	243	98.0
0.0022_1	216	241	97.2
0.0044_3	202	243	98.0
0.0088_5	210	242	97.6
0.033_2	190	245	98.8
0.049_8	186	245	98.8
0.066_4	170	242	97.6

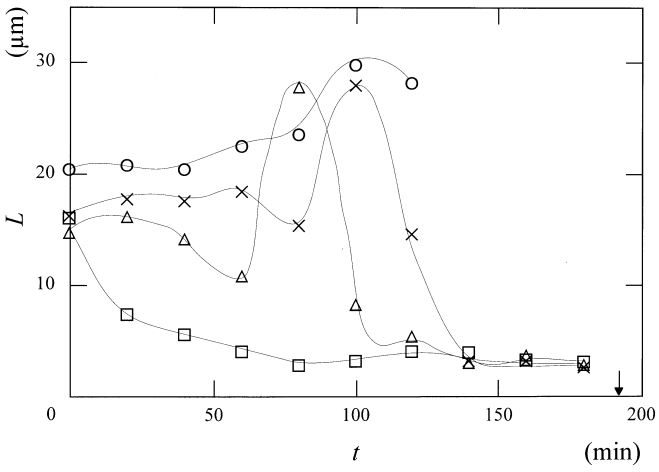

Fig. 8. Crystal size in the drying process of D1W52 spheres at 25 °C. In water, $\phi = 0.0332$, 0.05 ml. *Circles* from CCD observation, $r = 0$ mm, *crosses* from MCPD, $r = 0$ mm, *triangles* from MCPD, $r = 2.7$ mm, *squares* from MCPD, $r = 3.5$ mm. *Arrow* shows the T value

and 3. This value of the dried film is slightly larger by about 10% than the diameter of the colloidal spheres (88 nm). This shows that the neighbored spheres are very close but not in contact with each other keeping crystal-like structure. The reason why a slight difference occurs between the observed inter-sphere distance and the diameter is not clear yet. However, several reasons will be suggested. First, the film at $t = 12$ days still contains some water in the cavities of the film. Second, inter-sphere repulsive forces via electrical double layers in the suspension are still effective in the film. Third, expansion of the sphere size by the hairy chains of polystyrene at the sphere surfaces will occur in suspension. Fourth, the size determined with an electron microscope is smaller than the real size in suspension. Fifth, rather large errors must be considered for the assumption of several parameters, especially the dielectric constant of polystyrene spheres when Eq. 1 is used. It should be noted here that the spheres in the dried film of polystyrene spheres have been reported to distribute in the sphere contact and the closed-packed structure confirmed by the transmitted-light intensity measurement [36].

Figure 8 shows the change in the size of the single crystals in the course of drying, observed from the CCD pictures directly (open circles) and from the reflection spectroscopy using the half-width of the reflection peaks shown in Fig. 7. The former method gave L-values that were not so sensitive to time. However, the two methods gave values quite similar in magnitude to each other. It is interesting to note that the maximum values are observed in crystal size in the course of drying processes. The reason for this is the contamination of the sample drop with the surrounding carbon dioxide in air. It is highly plausible that the maximum peak exists for the film at $r = 3.5$ mm at a time less than the 20 min in Fig. 8.

Concluding remarks

Macroscopic spoke-like and ring-like cracks, broad ring patterns, and microscopic fractal patterns were observed for colloidal crystal suspensions of monodispersed polystyrene spheres in this work. These structures were surprisingly similar to those of colloidal crystal suspensions of silica spheres reported previously [29]. The former and the latter spheres are hydrophobic and hydrophilic, respectively, in their surface nature in aqueous suspensions. Thus, it is clear from this work that the surface nature of the spheres is not so essential for the formation of the dissipative structures. Recent work on the size dependency of the dissipative structures in the drying process [37] also supports the finding that the size of spheres is not so important for the pattern formation. Spherical shape itself will be essential instead.

Acknowledgements Drs. M. Komatsu and M. Hirai of Catalysts and Chemicals Ind. Co. (Tokyo and Kitakyusyu) are deeply thanked for providing the silica spheres. The Ministry of Education, Science, Sports, and Culture is thanked for grants-in-aid for Scientific Research on Priority Area (A) (11167241) and for Scientific Research (B) (11450367). T. O. appreciates deeply the late Professor Emeritus Sei Hachisu for his continual encouragement and comments on our work.

References

1. Vanderhoff W, van de Hul HJ, Tausk RJM, Overbeek JThG (1970) In: Goldfinger G (ed) Clean surfaces: Their preparation and characterization for interfacial studies. Dekker, New York
2. Hiltner PA, Papir YS, Krieger IM (1971) J Phys Chem 75:1881
3. Kose A, Ozaki M, Takano K, Kobayashi Y, Hachisu S (1973) J Colloid Interface Sci 44:330
4. Mitaku S, Ohtsuki T, Kishimoto A, Okano K (1980) Biophys Chem 11:411
5. Lindsay HM, Chaikin PM (1982) J Chem Phys 76:3774
6. Pieranski P (1983) Contemp Phys 24:25
7. Ottewill RH (1985) Ber Bunsenges Phys Chem 89:517
8. Aastuen DJW, Clark NA, Cotter LK, Ackerson BJ (1986) Phys Rev Lett 57:1733
9. Pusey PN, van Megen W (1986) Nature (London) 320:340
10. Okubo T (1988) Acc Chem Res 21:281
11. Okubo T (1997) Curr Topics Colloid Interf Sci 1:169
12. Vanderhoff JW (1973) J Polymer Sci Symp 41:155
13. Nicolis G, Prigogine I (1977) Self-organization in non-equilibrium systems. Wiley, New York

14. Cross MC, Hohenberg (1993) Rev Mod Phys 65:851
15. Ohara PC, Heath JR, Gelbart WM (1997) Angew Chem 109:1120
16. Ohara PC, Heath JR, Gelbart WM (1998) Langmuir 14:3418
17. Uno K, Hayashi K, Hayashi T, Ito K, Kitano H (1998) Colloid Polymer Sci 276:810
18. Gelbart WM, Sear RP, Heath JR, Chang S (1999) Faraday Discuss 112:299
19. Van Duffel B, Schoonheydt RA, Grim CPM, De Schryver FC (1999) Langmuir 15:7520
20. Maenosono S, Dushkin CD, Saita S, Yamaguchi Y (1999) Langmuir 15:957
21. Brock SL, Sanabria M, Suib SL, Urban V, Thiyagarajan P, Potter DI (1999) J Phys Chem 103: 7416
22. Nikoobakht B, Wang ZL, El-Sayed MA (2000) J Phys Chem 104:8635
23. Ge G, Brus L (2000) J Phys Chem 104:9573
24. Chen KM, Jiang X, LC Kimerling, Hammond PT (2000) Langmuir 16:7825
25. Lin XM, Jaenger HM, Sorensen CM, Klabunde (2001) J Phys Chem 105:3353
26. Kokkoli E, Zukoski CF (2001) Langmuir 17:369
27. Ung T, Liz-Marzan, Mulvaney (2001) J Phys Chem B 105:3441
28. Shimomura M, Sawadaishi T (2001) Current Opinion Coll Interf Sci 6:11
29. Okubo T, Okuda S, Kimura H (2002) Colloid Polymer Sci 280:454
30. Gunnars J, Stahle P, Wang TC (1997) Computational Mech 19:545
31. Colina H, Roux S (2000) Eur Phys J E 1:189
32. Okubo T, Kimura H, Kimura T, Hayakawa F, Shibata T (2002) (publication in preparation)
33. Latterini L, Blossey R, Hofkens J, Vanoppen P (1999) Langmuir 15:3582
34. Okubo T (1995) J Colloid Interf Sci 171:55
35. Falconer KJ (1985) The geometry of fractal sets, Cambridge Univ Press
36. Okubo T (1986) J Chem Soc Faraday Trans 1 82:3175
37. Okubo T, Kimura K, Yamada T (2002) (publication in preparation)